ICAS 2020 SHANGHAI
International Council of the Aeronautical Sciences
32nd Congress of the International Council of the Aeronautical Sciences
September 6-10, 2021
Pudong Shangri-La, Shanghai, China

OPTIMIZATION OF LONGITUDINAL CONTROL OF AN AGRICULTURAL UAV USING LQR-PID CONTROL

Andrew Gomes Pereira Sarmento[1], Alain Giacobini de Souza[1], Alexandre Muniz Neves[2], Luiz Carlos Sandoval Góes[1] & Roberto Gil Annes da Silva[1]

[1]Instituto Tecnológico de Aeronáutica (ITA)
[2]CENIC Aeronáutica

Abstract

In the development of automatic piloting systems nowadays, flight tests are required to validate operations and tuning of the control loops, making the process costly. For an optimal point of stability within a region of operation, this work aims to use the modern control technique of Linear Quadratic Regulator (LQR), with minimization through the Riccati equation for the optimization of Proportional, Integral, and Derivative (PID) control loops in longitudinal piloting. The aircraft considered for the flight tests was the C2 fixed-wing Unmanned Aerial Vehicles (UAV) used for agricultural purposes. The nonlinear model coefficients of the aircraft were acquired using well-known computational methods. The inertia properties were acquired through drawings made in Computer-Aided Design (CAD) with the Catia® software and the aerodynamic properties' estimation with the Omni3d® software. The aircraft's applied system was the Micropilot® LRC2 autopilot that has cascade PID control loops for altitude and trajectory control; however, the control loops tuning responsible for longitudinal movement are this work's main contribution. In parallel, a flight test campaign was carried out to collect data and tune the autopilot gains in flight by an empirical method based on Ziegler-Nichols' method. The gain data collected during the flights are used to compare the data obtained by the theoretical computer model of the aircraft. Different performances related to the gains obtained by the flight test and the PID control loops' optimization method through the LQR method are demonstrated with the non-linear model's application under the effects of disturbances. The main achieved results are about the minimum energy cost. This minimization in energy cost is due to the PID in-flight tuning that takes more energy in the actuators than the PID optimized with the LQR method, which proves to be a promising system for faster development of agricultural UAVs.

Keywords: System of control, UAV, Flight test, Micropilot

1. General Introduction

Currently, there are a range of difficulties for the application of pesticides in plantations using UAVs autonomously, such as ambient temperature, wind and atmospheric pressure. Optimization solutions of the application by several UAVs using genetic algorithm in the evaluation of the time windows are found in [6], as well as the correction of the trajectory angle through the estimation of the wind speed in real time of flight is proposed in [3]. Proposals for new technologies such as Internet of Things (IoT) can also be seen in [14], in which the objective was to speed up the update of environmental changes during flights.

However, missions in agricultural areas include more reserved requirements for autonomous flights with fixed-wing aircraft, such as passage altitudes between 5 and 15 meters, an average speed of 180 km/h and greater reliability for correcting atmospheric disturbances, mainly for the longitudinal dynamics of the aircraft. In order to comply with these requirements with the least time spent in tuning the control gains of the longitudinal loops, the optimization of the PID loops, internal to the Micropilot® LRC2 autopilot system, is proposed in this work, using the linear quadratic regulator (LQR).

1.1 The UAV

The C2 is a new and unique UAV, the result of the unmanned aircraft development project for the application of pesticides, conducted by CENIC Aeronáutica, with support from government foundation. The aircraft is designed in its structural architecture with the extensive use of light and advanced materials, based on Carbon Fiber Reinforced Plastic (CFRP), offering good flight performance and structural reliability. Its simplified dimensional properties can be seen in Table 1, as well as the aircraft during the flight campaign in Figure 1.

Table 1 – Dimensional properties.

Properties			
$Wingspan[m]$	$Length[m]$	$Height[m]$	$Weight[kg]$
5.000	2.863	1.080	60

Figure 1 – UAV C2.

2. Longitudinal models

For the creation of the model it was necessary to reproduce the aircraft by the panel method through the Omni3d® software, in which this model was used to estimate the coefficients responsible for the aerodynamic model, Figure 2b. On the other hand, it was also necessary to represent the aircraft in Computer-Aided Design (CAD), using the Catia® software, to estimate the moments and products of inertia used in the model, Figure 2a.

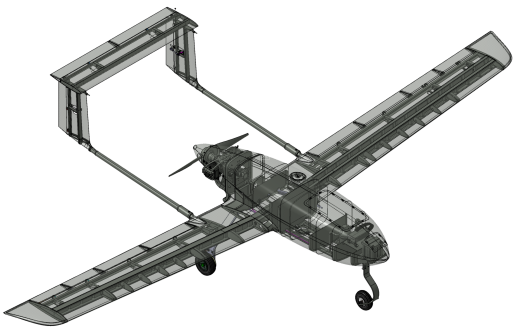

(a) UAV C2 CAD model.

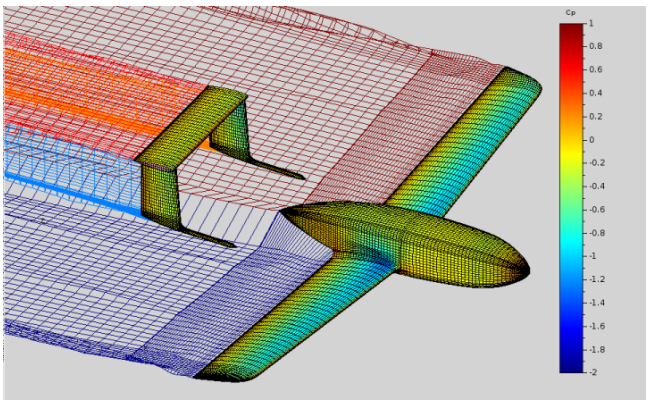

(b) UAV C2 panel model.

Figure 2 – Methods used to define the model.

2.1 Non-linear longitudinal model

The total non-linear model of the aircraft is simplified to decouple the longitudinal dynamics of the aircraft's lateral-directional and make only the equations referring to the longitudinal dynamics, some considerations are made about the lateral-directional variables, as described in Equations 1 and 2.

$$p = r = \phi = v = \psi = constant \tag{1}$$

$$\dot{p} = \dot{r} = \dot{\phi} = \dot{\psi} = \dot{v} = 0 \tag{2}$$

With the simplifications described above, the equations of the longitudinal nonlinear model can be represented by the differential equations responsible for the pitch rate (q), pitch angle (θ), velocities in the body system (u) and (w) and altitude (h), [13]. Variables taken from the inertia matrix such as (I_{xx}), forces and moments acting on the aircraft such as (F_x) and (M), are also considered in the motion equations, as can be seen from the equation 3 to the equation 12.

$$c_5 = \frac{I_{zz} - I_{xx}}{I_{yy}} \tag{3}$$

$$c_6 = \frac{I_{xz}}{I_{yy}} \tag{4}$$

$$c_7 = \frac{1}{I_{yy}} \tag{5}$$

$$\dot{u} = rv - qw - gsen(\theta) + F_x/m \tag{6}$$

$$\dot{w} = qu - pv + gcos(\phi)cos(\theta) + F_z/m \tag{7}$$

$$\dot{\alpha} = (u\dot{w} - w\dot{u})/(u^2 + w^2) \tag{8}$$

$$\dot{V} = (u\dot{u} + v\dot{v} + w\dot{w})/V \tag{9}$$

$$\dot{q} = c_5 pr - c_6(p^2 - r^2) + c_7 M \tag{10}$$

$$\dot{\theta} = qcos(\phi) - rsen(\phi) \tag{11}$$

$$\dot{h} = usen(\theta) - vsen(\phi)cos(\theta) - wcos(\phi)cos(\theta) \tag{12}$$

Thus, the observation or output equations can be deduced according to the previous simplifications, considering the effects of sensory errors, such as the terms (Δq) and ($\Delta\theta$) related to the polarization or bias terms of the observed measures. The sub-index ($_m$) identifies the variables actually measured. Equations 13 to 16.

$$q_m = q + \Delta q \tag{13}$$

$$\theta_m = \theta + \Delta\theta \tag{14}$$

$$h_m = h \tag{15}$$

$$V_{t,m} = \sqrt{u_t^2 + w_t^2} \tag{16}$$

2.2 Linearized longitudinal model

The linearized mathematical model used in the research is defined in the format of the equations 17 and 18, in which the matrix (A) is responsible for the dynamics of the states and the matrix (B) for the influence of the actuators on the states. The variables considered in the states are shown by the vector of the equation 19, as well as the throttle input, (δ_π) and elevator input, (δ_{el}), by the equation 20.

$$\dot{x} = Ax + Bu \tag{17}$$

$$y = cx \tag{18}$$

$$x = \begin{bmatrix} V & \alpha & \theta & q & h \end{bmatrix} \tag{19}$$

$$u = \begin{bmatrix} \delta_t & \delta_e \end{bmatrix} \tag{20}$$

The initial constants adopted to calculate the equilibrium condition for a straight-level flight of the C2 UAV were as follows: speed of 35 m/s at an altitude of 750 meters from sea level, the equilibrium results are shown by the equation 21.

$$\begin{bmatrix} V_e \\ \alpha_e \\ \theta_e \\ h_e \\ \delta_{t_e} \\ \delta_{e_e} \end{bmatrix} = \begin{bmatrix} 35m/s \\ -0,1564^o \\ -0,1564^o \\ 750m \\ 37,1\% \\ -0,3096^o \end{bmatrix} \tag{21}$$

Next, the linearized model in the equilibrium condition is described in Equations 22 and 23, where the matrices (A) and (B) are presented. The technique used is based on the Taylor series expansion, with the retention only of the linear term, as the higher-order terms of the Taylor series expansion are disregarded, these terms must be small enough, that is, the values of variables deviate only slightly from the operating condition, [10].

$$A = \begin{bmatrix} -0,1096 & 5,4712 & -9,8066 & 0,0201 & -0,000016 \\ -0,0160 & -4,0540 & 0 & 1,1870 & 0,000027 \\ 0 & 0 & 0 & 1,2857 & 0 \\ 0,0076 & -47,1705 & 0 & -7,4390 & -0,0001 \\ 0 & -35,0000 & 35,0000 & 0 & 0 \end{bmatrix} \tag{22}$$

$$B = \begin{bmatrix} 6,5165 & 0,1487 \\ 0,0005 & -0,2418 \\ 0 & 0 \\ 1,3220 & -38,0456 \\ 0 & 0 \end{bmatrix} \tag{23}$$

3. Longitudinal control loops

The flight control mode explored in this work is aimed at the cruising condition, aiming at the longitudinal characteristics of the UAV during the mission. For this, longitudinal control loops are defined in the PID and LQR architectures of longitudinal dynamics.

3.1 PID control loops

The longitudinals control loops implemented in the autopilot onboard the aircraft are responsible for the level flight mode that can maneuver the aircraft along the reference points defined during mission planning, maintaining the desired altitude. This mode of operation is composed of the control strategies in which the elevator control pitch angle, the pitch angle controls the altitude, and the engine throttle controls the flow velocity read by the Pitot tube. As shown in Figure 3.

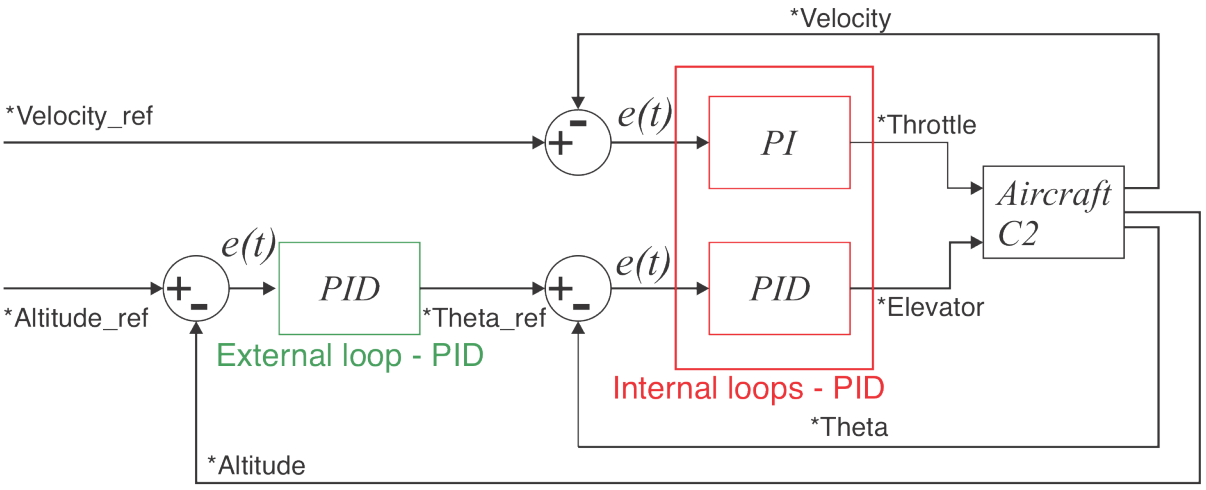

Figure 3 – PID longitudinal control loops.

3.2 LQR control loops

In order to carry out the optimization studies, a representation with the LQR architecture was proposed, in which its compensator is composed of a pure integrator, as well as two earnings matrices (L) responsible for the compensator and (K) by the states fed back. As shown in Figure 4.

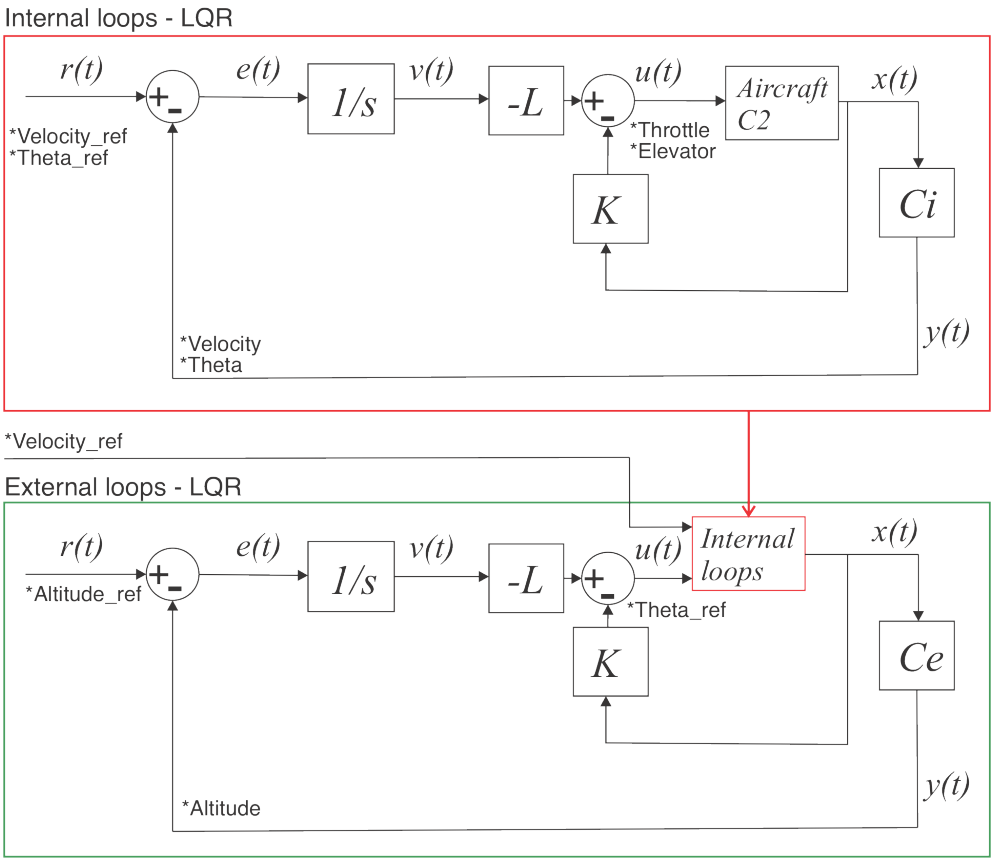

Figure 4 – LQR longitudinal control loops.

Subsequently, the gains from the LQR architecture (L and K) will be converted to the gains related to the PID controller (K_p, K_i and K_d).

4. In-flight tuning

The method adopted by the manufacturer for tuning the PID control loops of the Micropilot® LRC2 autopilot in flight is an adaptation of the Ziegler-Nichols method compared to that described in [10].

With the aircraft operational to start the in-flight tests, the process for tuning the control loops is done by observing the behavior of the aircraft and the data controlled during the flight. Repeating the process until an acceptable output performance from the control systems. The recommended order for tuning the control loops is found in [8] and defined in:

1. Elevator from pitch
2. Pitch from altitude
3. Throttle from airspeed

For the beginning of the control tuning, the initial gains used came from in-flight tests carried out by a smaller test aircraft of the Telemaster Senior model.
The tests proceeded with the placement of reference points using the command *fromTo* along the path formed between the reference points. The placement of these points was defined so that the aircraft does not leave the pilot's field of vision, ensuring the safety of the flight.
After planning the reference trajectory, the order in which the meshes will be adjusted is defined, that is:

1. Initially, the focus is on the elevator from the pitch loop, because if the internal loop is unstable the aircraft will oscillate quickly, more than 1 Hz during the maneuver. If the oscillate is consistent the pilot resumes the aircraft manual controller. For the isolation of this control loop from the rest of the system, it is recommended to put the aircraft in attitude arcade mode. The mode controls the attitudes through the radio control sticks, as well as engine power, see [7].
2. After that, tune the loops responsible for altitude and relative speed. The loops are most complicated to tune due to their coupling caused by the kinetic and potential energies related to the control variables. Because this reason, the gains referring to these two control loops are adjusted at the same time.

Following, the steps to tune each control loop are described below:

1. Starting with the term (P), the term is raised until the sustained oscillation of the movement, then reduced by 30% of the term in relation to the value observed during the oscillation;
2. The term (I) is increased until the aircraft is just below the point of instability and then reduced by around 5%;
3. The third component (D), was adjusted gradually increasing to increase the aircraft's phase margin and stability, always observing not to show oscillations.

The first tuning of the control loops was done following the steps above. However, despite the aircraft flying in a controlled manner, optimization of control gains is not guaranteed, as well as possible instability during the change in the balance point of the aircraft. In UAVs, the velocity read by the Pitot tube is the main variable of the model responsible for the change in the equilibrium point. To circumvent this problem, the autopilot is equipped with the stepped gain system, varying the gains of the PID loops with the different inputs of the airspeed values.
With the possibility of scaled gain, we opted for the LQR control architecture to calculate the gains in each equilibrium condition and later transform the control gains to the gains normally used in PID controllers. The LQR mesh methodology used to calculate gains from the longitudinal model is presented below.

5. LQR tuning

The adopted LQR architecture was adapted from [13], in which pure integrators were used as compensators to facilitate the relationship with the PID meshes implemented in autopilot, so the adapted architecture can be seen in Figure 5.

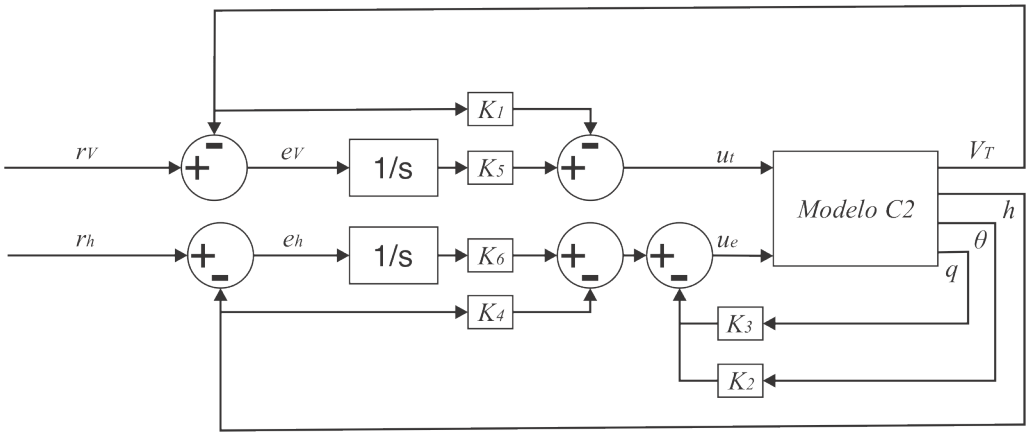

Figure 5 – Arquitetura de Controle LQR - Longitudinal. Fonte: adaptado de [13]

The states of the linearized model used for tuning the LQR mesh, as well as the inputs, are the same as described above. After using the solution of the Riccati equation 24, for the optimization of the LQR gains, the gains related to each part of the architecture are obtained, as described by the equation 25. The equation 26 the second column is totally null as the autopilot system has no angle of attack measurement (α) for the controllers.

$$A^T P + PA - (PB)R^{-1}(B^T P) + Q = 0 \tag{24}$$

$$K = R^{-1}(B^T P) = \begin{bmatrix} Ky & Kv \end{bmatrix} \tag{25}$$

$$Ky = \begin{bmatrix} K1 & 0 & 0 & 0 & 0 \\ 0 & 0 & K2 & K3 & K4 \end{bmatrix} \tag{26}$$

$$Kv = \begin{bmatrix} K5 & 0 \\ 0 & K6 \end{bmatrix} \tag{27}$$

6. LQR to PID

A method of converting the optimal gains tuned by the LQR method to the PID controller is initially proposed by [9] and later demonstrated with modifications in [1], [5] and [12].
The methodology was applied in the aeronautical environment in [2], with the optimal tuning of the Proportional Derivative (PD) control system in a multi-rotor, in [11] it is applied in the optimal tuning of the PID pitch control of an aircraft with a fixed-wing and in [4] was applied in the multi-loop PID tuning of the control of the internal loop and the altitude loop of a quadcopter.

6.1 The method

Considering the linearized model presented above and rearranging the LQR mesh compensator as a pure integrator, the augmented system as in Equation 28 and the augmented states of Equation 29, [9].

$$\dot{x}_a = \begin{bmatrix} A & 0 \\ C & 0 \end{bmatrix} \begin{bmatrix} x \\ w \end{bmatrix} + \begin{bmatrix} B \\ 0 \end{bmatrix} u \tag{28}$$

$$\bar{x} = \begin{bmatrix} x \\ w \end{bmatrix} \tag{29}$$

The system input (u) is written as shown in Equation 30, where the gains (K_p), (K_i) and (K_d) are related to the control architecture PID, [9].

$$u = -K_p y - K_i \int_0^t y dt - K_d \dot{y} \tag{30}$$

For simplification, Equation 30 is rewritten as in Equation 31.

$$u = -\bar{K}_p x - \bar{K}_i \int_0^t y dt \tag{31}$$

Where the gains ($\bar{K}_p$) and ($\bar{K}_i$) are defined in Equations 32 and 33. The component (I) represents an identity matrix.

$$\bar{K}_p = (I + K_d CB)^{-1}(K_p C + K_d CA) \tag{32}$$

$$\bar{K}_i = (I + K_d CB)^{-1} K_i \tag{33}$$

To obtain the desired controlled response, the matrices (Q) and (R) related to LQR optimization are defined. Next, the matrix ($\bar{P}$) is obtained, equation 34 resulting from the optimization solution, in which the part (P_{11}) is related to the states of the model and the part (P_{12}) is related to the integrator.

$$\bar{P} = \begin{bmatrix} P_{11} & P_{12} \\ P_{21} & P_{22} \end{bmatrix} \tag{34}$$

The optimal input to the system is given by the LQR solution, Equation 35.

$$u^* = -R^{-1}\bar{B}^T \bar{P}\bar{x} \tag{35}$$

From Equation 35, the relations between the gains of the LQR controller and the gains of the PID controller are defined through the rewriting of the Equations 32 and 33 in the Equations 36 and 37.

$$\bar{K}_p = R^{-1}B^T P_{11} \tag{36}$$

$$\bar{K}_i = R^{-1}B^T P_{12} \tag{37}$$

Because the components (K_p) and (K_d) are contained in the gain matrix ($\bar{K}_p$) and the component (K_i) is contained in the gain matrix ($\bar{K}_i$), the Equations 36 and 37 are rewritten as presented in Equations 39 and 40, considering the matrix ($\bar{C}$) as described in Equation 38.

$$\bar{C} = \begin{bmatrix} C \\ CA - CB\bar{K}_p \end{bmatrix} \tag{38}$$

$$\begin{bmatrix} K_p & K_d \end{bmatrix} = \bar{K}_p \bar{C}^{-1} \tag{39}$$

$$K_i = (I + K_d CB)\bar{K}_i \tag{40}$$

Thus, the components (K_p), (K_i) and (K_d) are obtained, represented for example in a MIMO system as in Equation 41.

$$K_p = \begin{bmatrix} K_{p11} & 0 & 0 \\ 0 & K_{p22} & 0 \\ 0 & 0 & K_{p33} \end{bmatrix} K_i = \begin{bmatrix} K_{i11} & 0 & 0 \\ 0 & K_{i22} & 0 \\ 0 & 0 & K_{i33} \end{bmatrix} K_d = \begin{bmatrix} K_{d11} & 0 & 0 \\ 0 & K_{d22} & 0 \\ 0 & 0 & K_{d33} \end{bmatrix} \tag{41}$$

7. Results

To obtain the gains of the internal and external loops using the LQR architecture the matrices (Q) and (R) are necessary. For defined the matrices in this work, it is were obtained recursively to improve the performance of the gains obtained by in-flight tuning. The weight matrices can be observed in the equations 42 to 45.

$$Q_{Internal} = diag\begin{bmatrix} 1 & 0 & 1200 & 3 & 0 & 2 & 10 \end{bmatrix} \tag{42}$$

$$R_{Internal} = diag\begin{bmatrix} 10 & 4 \end{bmatrix} \tag{43}$$

$$Q_{External} = diag\begin{bmatrix}0 & 0 & 0 & 0 & 1500 & 0 & 0 & 8\end{bmatrix} \tag{44}$$

$$R_{External} = diag\begin{bmatrix}100\end{bmatrix} \tag{45}$$

After some days for flight tests, adding a total of 36 hours dedicated to the tuning of the control gains, the resulting gains can be consulted in the Table 2, in the column referring to the $PID_{inflight}$. The gains arising from the tunings performed with the optimization using the LQR architecture are also shown in the Table 2.
It is notable that the gains referring to the speed maintenance control loop ($K_{p,t}$,$K_{i,t}$ and $K_{d,t}$), when obtained by the LQR methodology were smaller because during the choice of weights for optimization a slower engine response than that obtained during the in-flight tuning was sought. The other gains related to the altitude maintenance control loops were required for faster dynamics in the optimization by LQR, for this reason, their values were higher than those obtained in the in-flight tuning.

Table 2 – PID control gains.

	$PID_{inflight}$	PID_{LQR}
$K_{p,t}$	2.3500	0.9180
$K_{i,t}$	0.7800	0.9363
$K_{p,e}$	-3.3800	-15.3091
$K_{i,e}$	-0.8300	-1.2661
$K_{d,e}$	-0.8000	-0.9651
$K_{p,\theta}$	1.8300	3.9076
$K_{i,\theta}$	0.1200	0.2828
$K_{d,\theta}$	0.0200	0.4154

Applying the control gains obtained, in the non-linear longitudinal model of the UAV C2, with the reference speed reference equal to the balance, Figure 6 and the altitude reference entry simulating an altitude gain of 10 meters in 5 seconds and the loss of 5 meters of altitude in 5 seconds, Figure 7, it is remarkable that the behavior of the controllers tuned by LQR has similar behavior with the controllers tuned in in-flight tests.
In the Figure 6 it is noticeable oscillation during the beginning of the simulation caused by the non-linearities of the model, but it is also possible to notice oscillations in the times of 10, 15, 20, and 25 seconds, caused by the altitude transients, however, although the oscillation of the controller tuned by the LQR has a slower behavior concerning the one tuned in flight, the control via LQR gains manages to stabilize the speed in the reference, not requiring sudden changes in the motor-propulsive system.

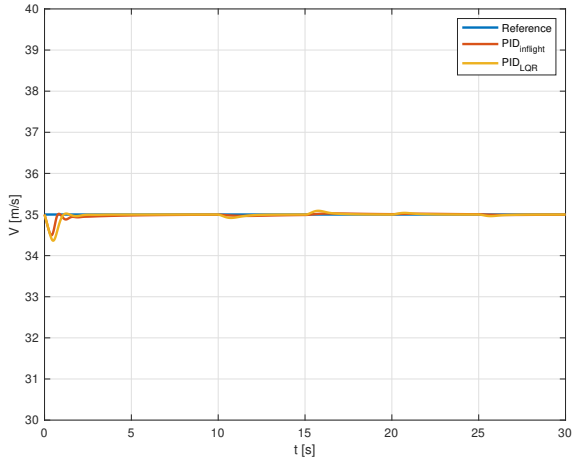

Figure 6 – Speed control loop results

On the other hand, with the increased response speed required in the LQR-optimized controller for altitude control, it is noticeable in the Figure 7 that the responses are faster and with less overshoot compared to the controller obtained in the flight tests, these differences are more visible in the transient periods. This phenomenon is caused by a faster performance and greater amplitude of the elevator control surface.

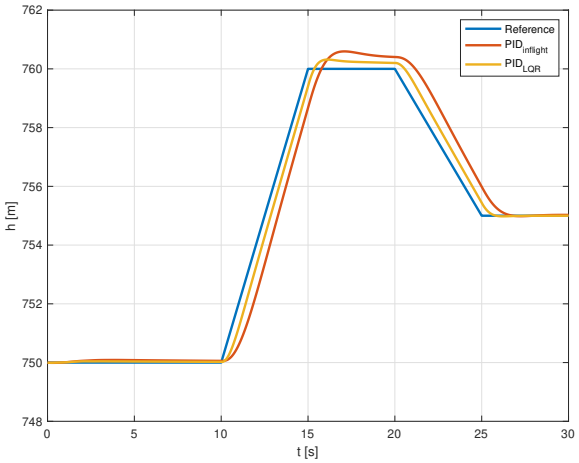

Figure 7 – Altitude control loop results

As before in altitude control, the pitch angle control also had the LQR optimization requirement to be faster and get less overshoot compared to the tuned in-flight controller. Because its reference is produced by the altitude control, two resulting references were obtained for the same altitude reference maneuver, however, it is possible to see in the Figure 8, that the LQR-optimized controller can follow almost faithfully its reference, on the other hand, the other controller presents a discrepancy between the reference values and the response of the controlled system.

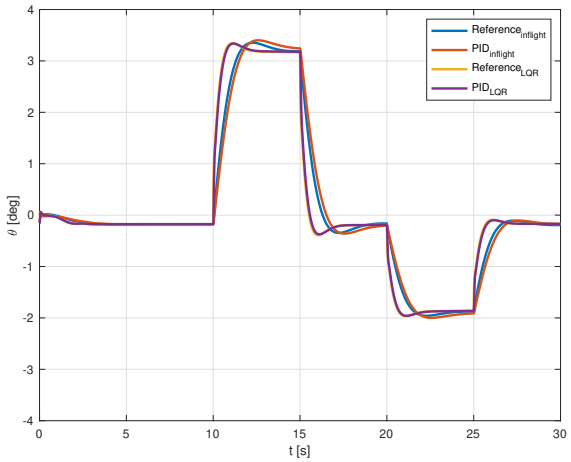

Figure 8 – Pitch angle control loop results

8. Conclusions and Future Work

It was possible to observe in the results that both methods of tuning the control loops are effective if used recursively, as they arrived in stable responses for the same reference maneuver, however, the tuning performed by the optimization method using LQR obtained a faster response, with less overshoot and consequently greater precision in maneuvers.
During the tuning process, with few hours of simulation in a computational environment, it is possible to make numerous tuning attempts using LQR optimization, this process ends up spending less time

and development cost, unlike what happens in in-flight tuning campaigns. However, for the LQR optimization method to work, a representative model of the aircraft is needed, obtained by advanced computational methods or even through parameter identification.
For future work, it is desirable to implement the gains resulting from LQR optimization in the autopilot, validating the method with real-world restrictions. It is also desirable to collect in-flight data from longitudinal variables. Consequently, for the total control of the aircraft, it is interesting to study the attitude control grids and lateral-directional guidance, for the application of such a method.

9. Acknowledgments

Thanks to the Aeronautical Technological Institute (ITA), in particular the Laboratory of Aeronautical Systems (LSA) for granting the necessary facilities and structure for the development of the work and to the National Council for Scientific and Technological Development (CNPQ) for financial support in the search.

10. Contact Author Email Address

Mailing address: Praça Marechal Eduardo Gomes, 50 Vila das Acácias, 12228-900, São José dos Campos/SP - Brazil.
Telephone number: +55 91 9 8144-8283.
Email: andrewgp@ita.br.

11. Copyright Statement

References

[1] Rosa Argelaguet, Montserrat Pons, Joseph Aguilar Martin, and Joseba Quevedo. A new tuning of PID controllers based on LQR optimization. *ECC 1997 - European Control Conference*, pages 1855–1859, 1997.

[2] Valeria Artale, Cristina L.R. Milazzo, Calogero Orlando, and Angela Ricciardello. Comparison of GA and PSO approaches for the direct and LQR tuning of a multirotor PD controller. *Journal of Industrial and Management Optimization*, 13(4):2067–2091, 2017.

[3] Matthew Coombes, Tom Fletcher, Wen Hua Chen, and Cunjia Liu. Optimal polygon decomposition for uav survey coverage path planning in wind. *Sensors (Switzerland)*, 18(7):1–28, 2018.

[4] Rafael Guardeño, Manuel J. López, and Víctor M. Sánchez. MIMO PID controller tuning method for quadrotor based on LQR/LQG theory. *Robotics*, 8(2):15–21, 2019.

[5] Jian Bo He, Qing Guo Wang, and Tong Heng Lee. PI/PID controller tuning via LQR approach. *Chemical Engineering Science*, 55(13):2429–2439, 2000.

[6] He Luo, Yanqiu Niu, Moning Zhu, Xiaoxuan Hu, and Huawei Ma. Optimization of Pesticide Spraying Tasks via Multi-UAVs Using Genetic Algorithm. *Mathematical Problems in Engineering*, 2017, 2017.

[7] Micropilot. MicroPilot MP2128^{LRC} Installation & Operation . Technical Report 26 January 2017, MicroPilot Inc., Stony Mountain, Manitoba - Canada, 2017.

[8] Micropilot. MicroPilot Autopilot Installation & Operation Manual. Technical Report 28 May 2018, MicroPilot Inc., Stony Mountain, Manitoba - Canada, 2018.

[9] S Mukhopadhyay. P.i.d. equivalent of optimal regulator. *Electronics Letters*, 14:1–2, 1978.

[10] Katsuhiko Ogata. *Engenharia de Controle Moderno*. Pearson, 2010.

[11] Surinder Singh Satbir Malik. LQR and Tuned PID Controller Design and Simulation for Aircraft Pitch Control Using MALTAB. *International Journal Of Scientific Research And Education*, 5(04):6291–6298, 2017.

[12] Saurabh Srivastava, Anuraag Misra, S. K. Thakur, and V. S. Pandit. An optimal PID controller via LQR for standard second order plus time delay systems. *ISA Transactions*, 60:244–253, 2016.

[13] B.L. Stevens, F.L. Lewis, and E.N. Johnson. *Aircraft Control and Simulation: Dynamics, Controls Design, and Autonomous Systems*. Wiley, 2015.

[14] Dimosthenis C. Tsouros, Stamatia Bibi, and Panagiotis G. Sarigiannidis. A review on UAV-based applications for precision agriculture. *Information (Switzerland)*, 10(11), 2019.